Published in final edited form as:
Ann Neurol. 2014 February ; 75(2): 255–265. doi:10.1002/ana.24086.

Abnormal Junctions and Permeability of Myelin in PMP22-Deficient Nerves

Jiasong Guo, PhD[2], **Leiming Wang, PhD**[1,2], **Yang Zhang, PhD**[2], **Jiawen Wu, PhD**[2], **Sezgi Arpag, MS**[2], **Bo Hu, MD, PhD**[2], **Beat A. Imhof, PhD**[3], **Xinxia Tian, PhD**[1], **Bruce D. Carter, PhD**[4], **Ueli Suter, PhD**[5], and **Jun Li, MD, PhD**[2,6]

[1]Department of Pathology, Peking University Health Science Center, Beijing, China [2]Department of Neurology, Center for Human Genetics Research, Vanderbilt Brain Institute, Vanderbilt University School of Medicine, Nashville, TN [3]Department of Pathology and Immunology, University of Geneva School of Medicine, Geneva, Switzerland [4]Department of Biochemistry, Vanderbilt University School of Medicine, Nashville, TN [5]Department of Biology, Institute of Molecular Health Sciences, ETH Zurich, Zurich, Switzerland [6]Tennessee Valley Healthcare System–Nashville VA, Nashville, TN

Abstract

Objective—The peripheral myelin protein-22 (*PMP22*) gene is associated with the most common types of inherited neuropathies, including hereditary neuropathy with liability to pressure palsies (HNPP) caused by PMP22 deficiency. However, the function of PMP22 has yet to be defined. Our previous study has shown that PMP22 deficiency causes an impaired propagation of nerve action potentials in the absence of demyelination. In the present study, we tested an alternative mechanism relating to myelin permeability.

Methods—Utilizing *Pmp22*$^{+/-}$ mice as a model of HNPP, we evaluated myelin junctions and their permeability using morphological, electrophysiological, and biochemical approaches.

Results—We show disruption of multiple types of cell junction complexes in peripheral nerve, resulting in increased permeability of myelin and impaired action potential propagation. We further demonstrate that PMP22 interacts with immunoglobulin domain–containing proteins known to regulate tight/adherens junctions and/or transmembrane adhesions, including junctional adhesion molecule-C (JAM-C) and myelin-associated glycoprotein (MAG). Deletion of *Jam-c* or *Mag* in mice recapitulates pathology in HNPP.

Interpretation—Our study reveals a novel mechanism by which PMP22 deficiency affects nerve conduction not through removal of myelin, but through disruption of myelin junctions.

Address correspondence to Dr Li, Department of Neurology, Vanderbilt University School of Medicine, 1161 21th Avenue South, Nashville, TN 37232. jun.li.2@vanderbilt.edu.
Current address for Dr Guo: Department of Histology and Embryology, Southern Medical University, Guang Zhou, China
J.G., L.W., and Y.Z. contributed equally.

Additional Supporting Information may be found in the online version of this article.

Potential Conflicts of Interest
Nothing to report.

Demyelination denudes axons and shunts depolarizing current out of nerve fibers, leading to either a reduction of conduction velocity or complete failure of action potential propagation. The latter is called *conduction block* and produces focal sensory/vision loss and limb paralysis. Nodes of Ranvier generate depolarizing currents 5× higher than the minimum required for the induction of an action potential. This excess is called the *safety factor*, which is greatly diminished once demyelination has occurred.[1]

Although the loss of myelin is widely regarded as one of the most important mechanisms that alter nerve conduction, effective nerve conduction is also thought to require a proper myelin seal through myelin junctions (such as tight junctions, adherens junctions).[2] These junctions seal the spaces between adjacent myelin lamellae as well as spaces between the myelin and axolemma.[2] In this study, we investigated this fundamental mechanism by utilizing a rodent model with peripheral myelin protein-22 (Pmp22) deficiency, in which we suspected an abnormality of myelin junctions.

Pmp22 is a tetra-span membrane protein that is primarily expressed in myelinating Schwann cells. A trisomy of human *PMP22* causes the most common inherited peripheral nerve disease, Charcot–Marie–Tooth disease type 1A. Solidifying the importance of this gene, heterozygous deletion of *PMP22* causes a different disorder, hereditary neuropathy with liability to pressure palsies (HNPP).[3] However, the precise biological role of PMP22 is largely unknown.

Patients with HNPP present with focal sensory loss and muscle weakness related to conduction block.[4] The hallmark pathology of HNPP is focal myelin thickenings known as *tomacula*.[5] Heterozygous inactivation of the *Pmp22* gene in mice (*Pmp22*$^{+/-}$) recapitulates the pathologic changes in patients with HNPP.[6] However, demyelination in *Pmp22*$^{+/-}$ mice does not occur until late stages of the disease, but nerve susceptibility to conduction block has been observed as early as 8 weeks of age.[6–8] This undermines the previously held assumption that demyelination is the cause of nerve conduction abnormalities in HNPP. In this study, we demonstrate that PMP22 deficiency disrupts the assembly of multiple types of myelin junction protein complexes. These junction abnormalities cause increased myelin permeability, which impairs propagation of action potentials.

Materials and Methods

Mouse and Genotyping

The *Pmp22*$^{+/-}$ mouse genotyping has been described.[6, 8] The institutional animal care and use committee at Vanderbilt University has approved the use of the animals.

K^+ Effect on Nerve Conduction

Mice anesthetized by isoflurane were allowed to acclimate to room temperature (22°C). One pair of stimulating electrodes was positioned percutaneously at the paraspinal site where the sciatic nerve forms most proximally. A needle recording electrode was inserted in the lateral gastrocnemius muscle. Recording from this proximal muscle showed negligible variations of compound muscle action potentials (CMAPs) among consecutive stimulations. In contrast, variations in CMAP were larger in the recordings from paw muscles. Minimal variations

were a prerequisite for observing the longitudinal effect of potassium. CMAP amplitudes were measured from peak to peak. A segment of sciatic nerve was wrapped in gauze that was soaked with 100mM KCl in Ringer's buffer or Ringer's buffer without added KCl. The solutions were refreshed every 3 minutes. For each CMAP, the stimulus intensity was verified as supramaximal. A baseline CMAP prior to the KCl or vehicle was collected. CMAP was then recorded every minute for 30 minutes. All subsequent CMAP amplitudes were normalized by the baseline CMAP to monitor the effect of KCl.

Myelin Permeability to Fluorescent Molecules

Myelin leakage was evaluated using 3 different procedures (see technical details in Fig 1A). The teased nerve fibers were imaged under a fluorescence microscope (Leica [Wetzlar, Germany] DM6000B). Nerve fibers from *Pmp22*$^{+/+}$ and *Pmp22*$^{+/-}$ mice were processed in identical conditions. Fluorescence intensity in the teased nerve fibers was quantified by placing a 5 × 5μm interest box 20μm away from the midline of the node of Ranvier. The image software (Leica AF2.5.0.6735) read the gray values from the interest boxes and calculated the mean density based on the gray values and the areas of the boxes. The final averaged values were derived from 105 *Pmp22*$^{+/+}$ fibers and 201 *Pmp22*$^{+/-}$ fibers.

For teased nerve fiber immunohistochemistry, Western blot, electron microscopy (EM), plasmids, epithelial cell culture, and evaluation of tight junction electrical resistance and coimmuno-precipitation (co-IP),[8–10] please see the Supplementary Materials.

Statistics

We compared continuous variables between 2 groups using Student *t* test. The difference among >2 groups was compared using 1-way analysis of variance if data were under normal distribution or Wilcoxon–Mann–Whitney test if data were not under normal distribution. Descriptive statistics were reported as means±standard deviation. The repeated-measures mixed-effects models were used to compare the mean change in the potassium experiments. Statistical analyses were performed using SAS9.3 and R3.0.0. Two-tailed probability values of <0.05 indicate statistical significance.

Results

Myelin Has Increased Permeability in Pmp22$^{+/-}$ Nerves

To test the permeability of the myelin, sciatic nerves with removal of epineurium were incubated with fluorescent molecules of various sizes (see Fig 1A and Materials and Methods for technical details). After 1 hour, there was a dramatic increase of fluorescein in *Pmp22*$^{+/-}$ nerve myelin, compared with that in *Pmp22*$^{+/+}$ nerve fibers (see Fig 1). This increase was quantitatively confirmed and was present even at the age of 6 weeks, prior to the occurrence of most tomacula between 3 and 6 months.[7, 8] The permeability was also increased for large sizes of dextran (70kD).

To exclude effects from hypoxia after nerve dissection, these dyes were locally injected into the sciatic nerves while mice were kept alive for 4 hours (see Fig 1A). Nerves were imaged,

and the same difference in myelin permeability was found between the *Pmp22*$^{+/+}$ and *Pmp22*$^{+/-}$ nerves (Supplementary Fig 1).

To determine the axolemmal integrity, distal sciatic nerves were crushed to allow the injected dyes to enter the transected axons and transport for 4 hours (see Fig 1A). Proximal segments 1cm away from the crushed site were examined. The fluorescent dyes were visible in axons but not in myelin (see Fig 1G1–3), suggesting that the axolemma in *Pmp22*$^{+/-}$ nerve fibers was intact.

The dye penetrance to myelin was not due to endocytosis, an issue that has been well addressed in a previous study.[11] Thus, our findings suggest abnormally increased myelin permeability in *Pmp22*$^{+/-}$-deficient nerves.

Abnormal Epineurium/Myelin Permeability Alters Nerve Conduction in Pmp22 Deficiency

To test the physiological effect of abnormal permeability, sciatic nerves in live animals were wrapped in gauze soaked with KCl (100mM) solution (Fig 2). Sciatic nerves were stimulated once every minute for a total of 30 minutes. CMAP following each stimulus was recorded at the medial gastrocnemius muscles. Similar approaches have been used to differentiate between intact peripheral nerves and nerves whose junctions are disrupted.[12–14] In these studies, pharmacological disruption of peripheral nerve junctions allows ions to penetrate epineurium and reach the periaxonal space to affect axonal potentials. In our studies, due to the tight seal, K^+ ions did not affect the wild-type nerve CMAP amplitude. In contrast, the K^+ ions significantly decreased the CMAP amplitude in *Pmp22*$^{+/-}$ nerves. This reduction was recoverable after K^+ ions were washed out, indicating that *Pmp22*$^{+/-}$ perineurium was highly permeable to K^+ ions. This is also consistent with the known Pmp22 expression in epineurium.[15]

Tight Junction Protein Complexes Are Disrupted in Pmp22$^{+/-}$ Nerves

To explain the increased myelin permeability, we evaluated tight junctions by teased nerve fiber immunostaining. Claudin-19, a principal protein of the peripheral nerve myelin tight junction, was identified in the *Pmp22*$^{+/+}$ paranodes, outer/inner mesaxons, and weakly in Schmidt–Lanterman incisures (SLIs; omitted in Fig 3). These distributions were fragmented or absent in *Pmp22*$^{+/-}$ nerves. In addition, claudin-19 was seen to accumulate in the perinuclear region and myelin of *Pmp22*$^{+/-}$ Schwann cells. Quantification confirmed more abnormalities in tomacula than in nontomaculous regions. These alterations were rarely observed in myelinated nerve fibers of wild type.

Abnormal distribution was also detected for other tight junction proteins, including zonula occludens 1 and 2 (ZO1 and ZO2; Supplementary Fig 2A–D).

Abnormal junction complexes were not a result of broadly altered expression levels of tight junction proteins. All proteins on Western blot showed levels similar to wild-type nerves, with the exception of claudin-5, which was increased in *Pmp22*$^{+/-}$ nerves compared to *Pmp22*$^{+/+}$ nerves (see Supplementary Fig 2E).

To determine whether Pmp22 deficiency affects the electrical resistance of tight junctions, mouse renal medullar epithelial cells were cultured to form a monolayer (see Fig 3). Tight junctions between these cells determine the electrical resistance across the monolayer (see Supplementary Materials for technical details).[16] Pmp22 has been localized within the intercellular junctions,[15] and thus its deficiency is expected to affect these tight junctions. Electrical resistance in *Pmp22*$^{+/-}$ junctions was significantly lower than in *Pmp22*$^{+/+}$ junctions. Furthermore, the junctions revealed by ZO2 immunostaining were disrupted in *Pmp22*$^{+/-}$ cultures.

Taken together, these results are consistent with an abnormal localization and function of tight junction complexes in Pmp22-deficient myelin.

Transmembrane Adhesion Proteins Are Mislocalized in Pmp22$^{+/-}$ Nerves

Studies have shown that tomaculalike structures can be recapitulated by deleting any of 4 genes: *Jam-c, Mag, Pten*, and periaxin.[17–20] Reliable periaxin antibodies were not available, Pten and its downstream signaling molecule (Akt) were unchanged in Western blot and immunostaining of *Pmp22*$^{+/-}$ nerves (Supplementary Fig 3).

Jam-c is a junction protein involved in transmembrane adhesion and regulates tight/adherens junctions. [17, 21, 22] Jam-c was detected in paranodes and SLIs in teased nerve fibers of 5-month-old *Pmp22*$^{+/+}$ mice. However, in *Pmp22*$^{+/-}$ paranodes, Jam-c was either reduced or absent, whereas the staining pattern appeared to be normal in *Pmp22*$^{+/-}$ SLIs (Fig 4). We quantitatively confirmed the loss of Jam-c in *Pmp22*$^{+/-}$ paranodes.

In younger *Pmp22*$^{+/-}$ nerves (3 months old), percentages of Jam-c–positive paranodes/SLIs were normal, including the total level of Jam-c (see Fig 4). Therefore, we compressed the sciatic nerve with a vessel clamp for 30 minutes.[8] Injuries have been shown to accelerate the removal of junction proteins in the nerves distal to the injury.[23] We reasoned that paranodes/SLIs with a lower abundance of Jam-c should lose their staining quicker than those with normal expression. Moreover, because patients with HNPP are particularly susceptible to paralysis following a nerve compression (hence the “pressure palsy” designation), any junctions that exist in *Pmp22*$^{+/-}$ nerves may be unstable. Compression induced the disappearance of Jam-c in the *Pmp22*$^{+/-}$ paranodes/SLIs more severely than in *Pmp22*$^{+/+}$ nerves. Similar changes were also observed for Mag staining in 3-month-old *Pmp22*$^{+/-}$ nerves.

Jam-c has been implicated in the formation of adherens junctions in dermal fibroblasts.[24] E-cadherin, a marker of adherens junctions,[25] was decreased in naive *Pmp22*$^{+/-}$ paranodes/SLIs (see Fig 4I). Following nerve compression, E-cadherins were hardly visible. We further examined the adherens junctions under EM as we have described.[25] Adherens junctions were significantly decreased in *Pmp22*$^{+/-}$ nerves compared to *Pmp22*$^{+/+}$ nerves (Supplementary Fig 4A–D). Interestingly, a similar change was also noticed in junctions between epineurial cells (see Supplementary Fig 4E, F).

In contrast, the paranodal septate junction proteins, contactin-associated protein (Caspr) and neurofascin, appeared to be similar between *Pmp22*$^{+/+}$ and *Pmp22*$^{+/-}$ mice in both naive and compressed nerves (see Supplementary Fig 4G1–J3).

Taken together, these findings suggest that Pmp22 deficiency alters multiple types of myelin junction complexes.

PMP22 Interacts with Transmembrane Adhesion Proteins

Tomacula develops in the peripheral nerves in the absence of Jam-c or Mag.[17, 18] These proteins interact or regulate tight/adherens junction proteins.[21, 26] Both Jam-c and Mag were reduced in *Pmp22*$^{+/-}$ paranodes/SLIs (see Fig 4), leading to speculation that Pmp22 may interact with Jam-c and/or Mag. We performed co-IP by coexpressing human PMP22 and JAM-C or MAG in HEK293 cells. The results demonstrate an interaction between PMP22 and JAM-C and between PMP22 and MAG (Fig 5). This interaction is dependent on the extracellular immunoglobulin (Ig) domain because deletion of the Ig domain of JAM-C, but not the intracellular domain of JAM-C, disrupted this interaction (*arrow* in Fig 5B). Moreover, the interaction between endogenous Pmp22 and Mag was also detectable in mouse sciatic nerves. However, our experiments showed no interaction between PMP22 and AZGP1 (an Ig domain protein in adipocytes for lipid degradation), or between PMP22 and ZO2[27] (Supplementary Fig 5).

The interaction between PMP22 and JAM-C/MAG raises an intriguing question. Jam-c and Mag are expressed in noncompact myelin,[17, 18] whereas Pmp22 is expressed in compact myelin. This led us to question how they might interact. We speculated that these proteins may overlap during development, but segregate to different domains in mature myelin. We then performed immunostaining. Up to postnatal day 20 (P20), Mag was partially colocalized with Pmp22 in immature internodes, paranodes, and SLIs (*arrows* in Fig 6A1–E3). By P30, Mag and Pmp22 were confined to their separate compartments (see Fig 6F1, G3). In line with this finding, interactions between endogenous Pmp22 and Mag were detectable by co-IP in mouse sciatic nerves at the age of P9, but not in adult nerves (see Fig 5D).

Together, these findings provide a molecular basis regarding how PMP22 may affect the assembly of junction protein complexes through protein–protein interactions.

Discussion

This study shows that Pmp22 deficiency disrupts and/or destabilizes multiple myelin junction protein complexes and profoundly increases the permeability of myelin. Abnormal permeability of myelin appears to affect the propagation of action potentials, because CMAP amplitude in *Pmp22*$^{+/-}$ nerves can be reduced by external application of K^+ ions. Although myelin is present in *Pmp22*$^{+/-}$ nerves, this increased permeability of myelin impairs its electrical seal and is functionally comparable to demyelination.

Identification of PMP22 interactions with Ig domain proteins may be pathogenically relevant. First, Jam-c and Mag are either reduced or missing in a portion of *Pmp22*$^{+/-}$

paranodes/SLIs. Second, ablation of either *Jam-c* or *Mag* results in tomacula similar to those in *Pmp22*$^{+/-}$ nerves.[17, 18] Jam-c has been shown to interact directly with ZO1/ZO2.[21] Thus, mislocalized Jam-c could contribute to the mislocalization of ZO1/ZO2 in *Pmp22*$^{+/-}$ nerves, and affects tight/adherens junctions.[28] Third, our previous study has demonstrated that *Mag*$^{-/-}$ nerves, like *Pmp22*$^{+/-}$ nerves, exhibit susceptibility to conduction block.[8] Fourth, the decrease of Ig domain proteins in *Pmp22*$^{+/-}$ paranodes would affect myelin lamellar adhesion between paranodal loops. This view is supported by literature demonstrating the loosened lamellar adhesion in *Pmp22*$^{+/-}$ paranodal tomacula.[29] Ablation of Jam-c also results in looser adhesion between adjacent paranodal lamellae.[17] This may increase the size of pathway-3 (illustrated in Fig 6H, I), which is a recently described pathway affecting myelin permeability.[11]

At present, it is unclear how Pmp22 deficiency affects the assembly of junction protein complexes through protein–protein interactions during development. However, roughly half the amount of Pmp22 is produced in *Pmp22*$^{+/-}$ nerves. Some junction complexes are still formed, but unstable. They are dislocated during aging (Jam-c was normal at 3 months, but reduced at 5 months; see Fig 4). This finding is consistent with minor pathology with normal conduction velocity in younger nerves (<8 weeks old).[8] However, abnormal myelin permeability is still present in these young nerves (see Fig 1E1–4) and explains their susceptibility to develop conduction block.[8]

Interestingly, heterozygous knockouts of *Jam-c* or *Mag* have normal phenotypes. Only homozygous knockout of the proteins causes tomacula. In addition, ablation of *claudin-19* eliminates tight junctions in peripheral nerve myelin, yet this results in minimal abnormalities in nerve conduction.[30] These observations are well in line with the finding that PMP22 affects multiple types of myelin junctions, leading to a strong effect on myelin permeability (see diagram in Fig 6H, I).

This mechanism may involve junctions in the epi-/perineurium, because Pmp22, Jam-c, and claudin-5 are all expressed in epi-/perineurial junctions.[15, 31] There are morphological changes of junctions between epineurial cells (see Supplementary Fig 4E, F). K^+ ions were able to reduce action potential propagation after being externally applied to *Pmp22*$^{+/-}$ nerves (see Fig 2). Epi-/perineurial junctions, as the initial barrier before K^+ accesses the periaxonal spaces,[12, 13] would have to become excessively permeable to the ions in *Pmp22*$^{+/-}$ epi-/perineurium.

Axonal constrictions in the tomacula may impair action potential propagation.[8] However, we observed an increase of myelin permeability (see Fig 1 E1–4) and susceptibility to conduction block prior to the onset of tomacula/ axonal constrictions in *Pmp22*$^{+/-}$ and *Mag*$^{-/-}$ nerves.[8] Therefore, abnormal myelin permeability is sufficient to impair action potential propagation in HNPP, independent of axonal constriction.

In summary, our study provides a novel mechanism that may affect nerve conduction in HNPP. Deficiency of Pmp22 dislocates junction protein complexes (see Fig 6H, I), thereby resulting in excessively permeable myelin, which impairs action potential propagation in the absence of demyelination.

Supplementary Material

Refer to Web version on PubMed Central for supplementary material.

Acknowledgments

This research is supported by grants from the NIH National Institute of Neurologic Disorders and Stroke (R01NS066927 to J.L. and R01NS064278 to B.D.C.), and a generous private fund from the Prinzmetal family. Work in our laboratory was also supported by the Swiss National Science Foundation. L.W. is a PhD candidate who has been supported by the China Scholarship Council (2011601075).

We thank Drs C. Sanders, A. Gow, and S. Scherer for their valuable comments on this study; A. Hamilton and J. Zou for their technical assistance; and Drs M. Furuse and P. Brophy for providing claudin-19 and neurofascin antibodies.

References

1. Kaji R, Bostock H, Kohara N, et al. Activity-dependent conduction block in multifocal motor neuropathy. Brain. 2000; 123(pt 8):1602–1611. [PubMed: 10908190]
2. Hartline DK, Colman DR. Rapid conduction and the evolution of giant axons and myelinated fibers. Curr Biol. 2007; 17:R29–R35. [PubMed: 17208176]
3. Li J, Parker B, Martyn C, et al. The PMP22 gene and its related diseases. Mol Neurobiol. 2013; 47:673–698. [PubMed: 23224996]
4. Li J, Krajewski K, Lewis RA, et al. Loss-of-function phenotype of hereditary neuropathy with liability to pressure palsies. Muscle Nerve. 2004; 29:205–210. [PubMed: 14755484]
5. Tyson J, Malcolm S, Thomas PK, et al. Deletions of chromosome 17p11.2 in multifocal neuropathies. Ann Neurol. 1996; 39:180–186. [PubMed: 8967749]
6. Adlkofer K, Martini R, Aguzzi A, et al. Hypermyelination and demyelinating peripheral neuropathy in Pmp22-deficient mice. Nat Genet. 1995; 11:274–280. [PubMed: 7581450]
7. Adlkofer K, Frei R, Neuberg DH, et al. Heterozygous peripheral myelin protein 22-deficient mice are affected by a progressive demyelinating tomaculous neuropathy. J Neurosci. 1997; 17:4662–4671. [PubMed: 9169527]
8. Bai Y, Zhang X, Katona I, et al. Conduction block in PMP22 deficiency. J Neurosci. 2010; 30:600–608. [PubMed: 20071523]
9. Zhang X, Chow CY, Sahenk Z, et al. Mutation of FIG4 causes a rapidly progressive, asymmetric neuronal degeneration. Brain. 2008; 131:1990–2001. [PubMed: 18556664]
10. Guo J, Ma YH, Yan Q, et al. Fig4 expression in the rodent nervous system and its potential role in preventing abnormal lysosomal accumulation. J Neuropathol Exp Neurol. 2012; 71:28–39. [PubMed: 22157617]
11. Mierzwa A, Shroff S, Rosenbluth J. Permeability of the paranodal junction of myelinated nerve fibers. J Neurosci. 2010; 30:15962–15968. [PubMed: 21106834]
12. Todd BA, Inman C, Sedgwick EM, et al. Ionic permeability of the frog sciatic nerve perineurium: parallel studies of potassium and lanthanum penetration using electrophysiological and electron microscopic techniques. J Neurocytol. 2000; 29:551–567. [PubMed: 11283412]
13. Todd BA, Inman C, Sedgwick EM, et al. Ionic permeability of the opossum sciatic nerve perineurium, examined using electrophysiological and electron microscopic techniques. Brain Res. 2000; 867:223–231. [PubMed: 10837817]
14. Hackel D, Krug SM, Sauer RS, et al. Transient opening of the perineurial barrier for analgesic drug delivery. Proc Natl Acad Sci U S A. 2012; 109:E2018–E2027. [PubMed: 22733753]
15. Notterpek L, Roux KJ, Amici SA, et al. Peripheral myelin protein 22 is a constituent of intercellular junctions in epithelia. Proc Natl Acad Sci U S A. 2001; 98:14404–14409. [PubMed: 11717414]
16. Masuda S, Oda Y, Sasaki H, et al. LSR defines cell corners for tricellular tight junction formation in epithelial cells. J Cell Sci. 2011; 124:548–555. [PubMed: 21245199]

17. Scheiermann C, Meda P, Aurrand-Lions M, et al. Expression and function of junctional adhesion molecule-C in myelinated peripheral nerves. Science. 2007; 318:1472–1475. [PubMed: 18048693]
18. Yin X, Crawford TO, Griffin JW, et al. Myelin-associated glycoprotein is a myelin signal that modulates the caliber of myelinated axons. J Neurosci. 1998; 18:1953–1962. [PubMed: 9482781]
19. Goebbels S, Oltrogge JH, Wolfer S, et al. Genetic disruption of Pten in a novel mouse model of tomaculous neuropathy. EMBO Mol Med. 2012; 4:486–499. [PubMed: 22488882]
20. Gillespie CS, Sherman DL, Fleetwood-Walker SM, et al. Peripheral demyelination and neuropathic pain behavior in periaxin-deficient mice. Neuron. 2000; 26:523–531. [PubMed: 10839370]
21. Ebnet K, Schulz CU, Meyer zu Brickwedde MK, et al. Junctional adhesion molecule interacts with the PDZ domain-containing proteins AF-6 and ZO-1. J Biol Chem. 2000; 275:27979–27988. [PubMed: 10856295]
22. Mandicourt G, Iden S, Ebnet K, et al. JAM-C regulates tight junctions and integrin-mediated cell adhesion and migration. J Biol Chem. 2007; 282:1830–1837. [PubMed: 17099249]
23. Jung J, Cai W, Lee HK, et al. Actin polymerization is essential for myelin sheath fragmentation during Wallerian degeneration. J Neurosci. 2011; 31:2009–2015. [PubMed: 21307239]
24. Morris AP, Tawil A, Berkova Z, et al. Junctional adhesion molecules (JAMs) are differentially expressed in fibroblasts and colocalize with ZO-1 to adherens-like junctions. Cell Commun Adhes. 2006; 13:233–247. [PubMed: 16916751]
25. Young P, Boussadia O, Berger P, et al. E-cadherin is required for the correct formation of autotypic adherens junctions of the outer mesaxon but not for the integrity of myelinated fibers of peripheral nerves. Mol Cell Neurosci. 2002; 21:341–351. [PubMed: 12401452]
26. Ebnet K. Organization of multiprotein complexes at cell-cell junctions. Histochem Cell Biol. 2008; 130:1–20. [PubMed: 18365233]
27. Tisdale MJ. Zinc-alpha2-glycoprotein in cachexia and obesity. Curr Opin Support Palliat Care. 2009; 3:288–293. [PubMed: 19823091]
28. Hartsock A, Nelson WJ. Adherens and tight junctions: structure, function and connections to the actin cytoskeleton. Biochim Biophys Acta. 2008; 1778:660–669. [PubMed: 17854762]
29. Madrid R, Bradley G. The pathology of neuropathies with focal thickening of the myelin sheath (tomaculous neuropathy): studies on the formation of the abnormal myelin sheath. J Neurol Sci. 1975; 25:415–448.
30. Miyamoto T, Morita K, Takemoto D, et al. Tight junctions in Schwann cells of peripheral myelinated axons: a lesson from claudin-19-deficient mice. J Cell Biol. 2005; 169:527–538. [PubMed: 15883201]
31. Colom B, Poitelon Y, Huang W, et al. Schwann cell-specific JAMC- deficient mice reveal novel expression and functions for JAM-C in peripheral nerves. FASEB J. 2012; 26:1064–1076. [PubMed: 22090315]
32. Balda MS, Whitney JA, Flores C, et al. Functional dissociation of paracellular permeability and transepithelial electrical resistance and disruption of the apical-basolateral intramembrane diffusion barrier by expression of a mutant tight junction membrane protein. J Cell Biol. 1996; 134:1031–1049. [PubMed: 8769425]

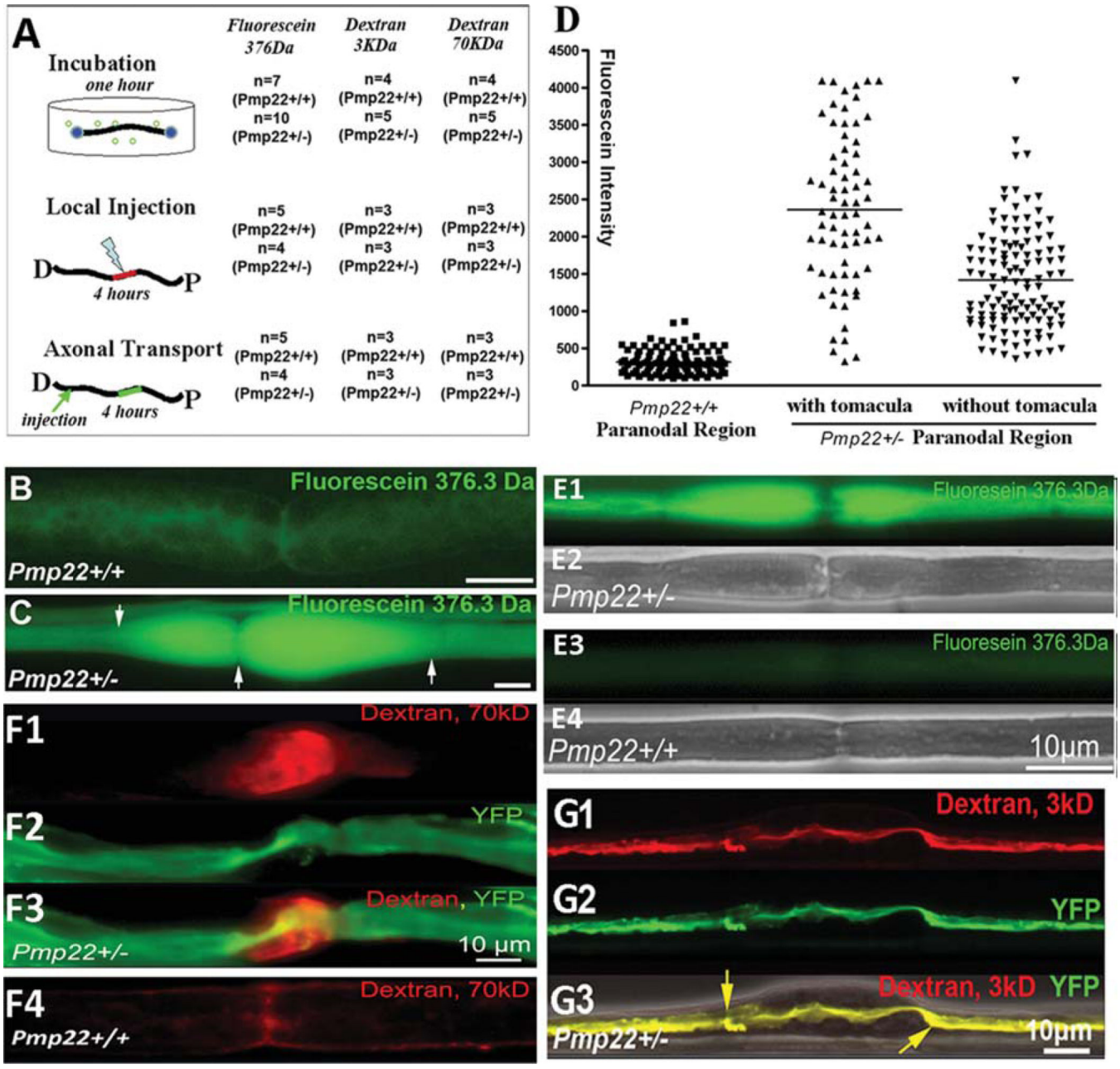

FIGURE 1.

Increase of myelin leakage in Pmp22$^{+/-}$ nerve fibers. Experiments were done in 24 Pmp22$^{+/-}$ mice and 15 *Pmp22*$^{+/+}$ mice at 10 to 11 months of age. In addition, the key findings in B–D were replicated in 6-week-old mice (3 *Pmp22*$^{+/+}$ and 3 *Pmp22*$^{+/-}$ mice; E1–4). (A) A diagram shows 3 different procedures that were used to evaluate myelin leakage. In the first procedure, 1cm sciatic nerve fascicles were submerged in artificial cerebrospinal fluid (aCSF; 10mM HEPES, 110mM NaCl, 17.8mM $NaHCO_3$, 4mM $MgSO_4$, 3.9mM KCl, 3mM KH_2PO_4, 1.2mM $CaCl_2$, and 10mM dextrose) after epineurium removal. Nerves were sealed at both ends with Vaseline. Three different sizes of fluorescence molecules (fluorescein 376Da from Sigma, St Louis, MO; 3kDa and 70kDa dextran from Molecular

Probes, Eugene, OR) were added (10mg fluorescein/ml aCSF; 2 or 5 mg/ml for 3 or 70 KDa dextran) for a 1-hour incubation at room temperature without oxygenation. Following a brief wash, the nerve fascicle was fixed in 4% paraformaldehyde for 5 minutes and teased into individual nerve fibers for fluorescence microscopy. In the second procedure, a 10ll Hamilton syringe connected with a glass pipette tip (diameter = 50lm) was used to inject 5ll fluorescence dyes into the sciatic nerves 5mm proximal to the sciatic nerve bifurcation. The injected mice were kept alive for 4 hours while anesthetized with tribromoethanol (Avertin). A 5mm sciatic nerve fascicle with injected dyes was then fixed and teased. In the third procedure, the sciatic nerve was injected with the dyes. The nerve was crushed with #5 Diamond forceps for 5 seconds to allow dyes to enter the transected axons. Mice were kept alive for 4 hours. A 5mm nerve fascicle 10mm proximal to the crushed site was processed for microscopic evaluation. (B) A teased nerve fiber from a *Pmp22*$^{+/+}$ mouse showed weak fluorescence after incubation with fluorescein. (C) Fluorescein molecules were drastically increased in *Pmp22*$^{+/-}$ nerve fibers, particularly in the tomaculous region (between *arrows*). (D) Fluorescence (fluorescein) intensity in the incubated nerves was quantified as described in Materials and Methods. The intensity was significantly increased in *Pmp22*$^{+/-}$ nerve fibers compared to *Pmp22*$^{+/+}$ nerve fibers (n = 105 *Pmp22*$^{+/+}$ nerve fibers from 7 mice, n = 69 *Pmp22*$^{+/-}$ fibers from 10 mice with counts in tomaculous region, n = 122 *Pmp22*$^{+/-}$ fibers from 10 mice with counts in nontomaculous region; $p < 0.001$). (E1–E4) Fluorescein was incubated with nerves from 6-week-old mice. A similar difference of fluorescent intensity was observed between *Pmp22*$^{+/+}$ and *Pmp22*$^{+/-}$ nerves. E2 and E4 were phase-contrast images. (F1–F4) To determine whether *Pmp22*$^{+/-}$ myelin is permeable to larger sizes of molecules, nerves from mice at 10 to 11 months of age were incubated with 70kD dextran. (F1) Strong fluorescence was visible in the paranodal myelin. (F2) Axon was labeled by yellow fluorescent protein (YFP) that was expressed from a transgene under a neuronal specific promoter.[8] (F4) In contrast, fluorescence in *Pmp22*$^{+/+}$ nerve fibers was minimal. (G1–G3) The 3kD dextran was taken up by the transected axons and transported in retrograde. The dextran was confined within the *Pmp22*$^{+/-}$ axon 10mm proximal to the transected site, including the axon within the tomaculous region (between *arrows* in G3). (G3) Axon was labeled by YFP overlapped with dextran, suggesting no fluorescence molecules leaking out of the axon. An overlaid phase-contrast image shows the location of tomacula.

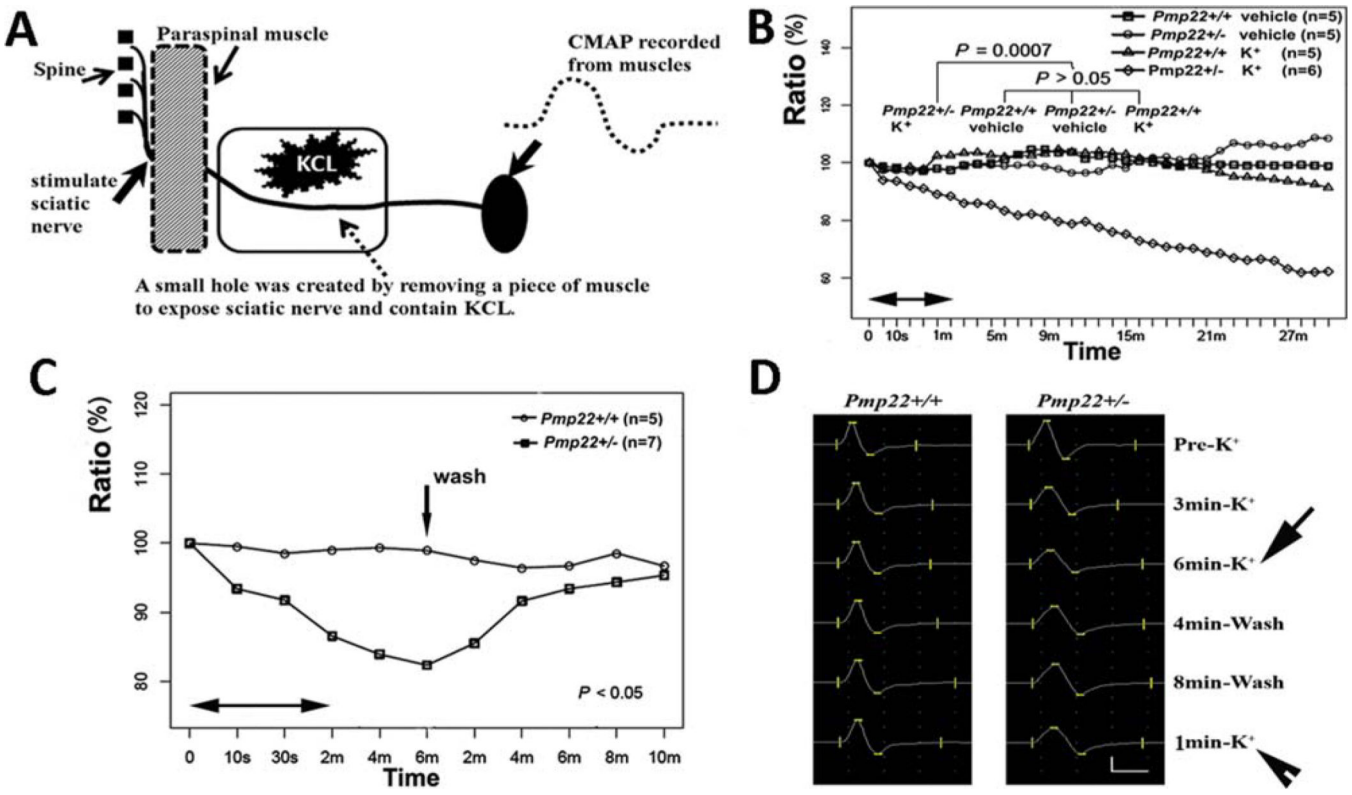

FIGURE 2.

Pmp22 deficiency increases myelin permeability. (A) Diagram showing the experimental setting for evaluating K^+ permeability of sciatic nerves. Please see additional details in Materials and Methods. (B) As marked in the figure, there were 4 experimental groups. Treatment of 100mM KCl in *Pmp22*$^{+/+}$ mice did not significantly alter compound muscle action potential (CMAP) amplitudes, compared with *Pmp22*$^{+/+}$ or *Pmp22*$^{+/-}$ mice treated with the vehicle. In contrast, treatment of 100mM KCl in *Pmp22*$^{+/-}$ mice caused a rapid decrease of CMAP amplitudes (n = 10 *Pmp22*$^{+/+}$ mice, n = 11 *Pmp22*$^{+/-}$ mice). The difference between the *Pmp22*$^{+/-}$ K^+ group and the other 3 groups was statistically significant ($p = 0.0007$). Note that within the first minute (between the 2 arrows), time points were not evenly scaled, but simply marked the points at 5, 10, 20, and 30 seconds. This was to show the rapid initial changes. (C) An experiment identical to that in B was performed to induce a reduction of CMAP by 100mM KCl ($p < 0.05$). However, at the 6th minute after the KCl application, KCl was washed out by Ringer's buffer (*vertical arrow* in C). CMAP quickly recovered. Again, within the first 2 minutes (between the 2 *horizontal arrows*), time points were not evenly scaled, but simply marked the points at 0, 10, and 30 seconds. (D) A specific example was made from a *Pmp22*$^{+/+}$ mouse and a *Pmp22*$^{+/-}$ mouse. CMAP remained constant in the *Pmp22*$^{+/+}$ mouse after KCl application (left column). In contrast, CMAP in the *Pmp22*$^{+/-}$ mouse was decreased from pre-K^+ 25.6 to 15.2mV after K^+ application (*arrow* in the right column). The CMAP recovered to 21.0mV after the K^+ washed out for 8 minutes. However, the 21.0mV CMAP was reduced to 17.6mV 1 minute after the second K^+ application *(arrowhead)*. [Color figure can be viewed in the online issue, which is available at wileyonlinelibrary.com.]

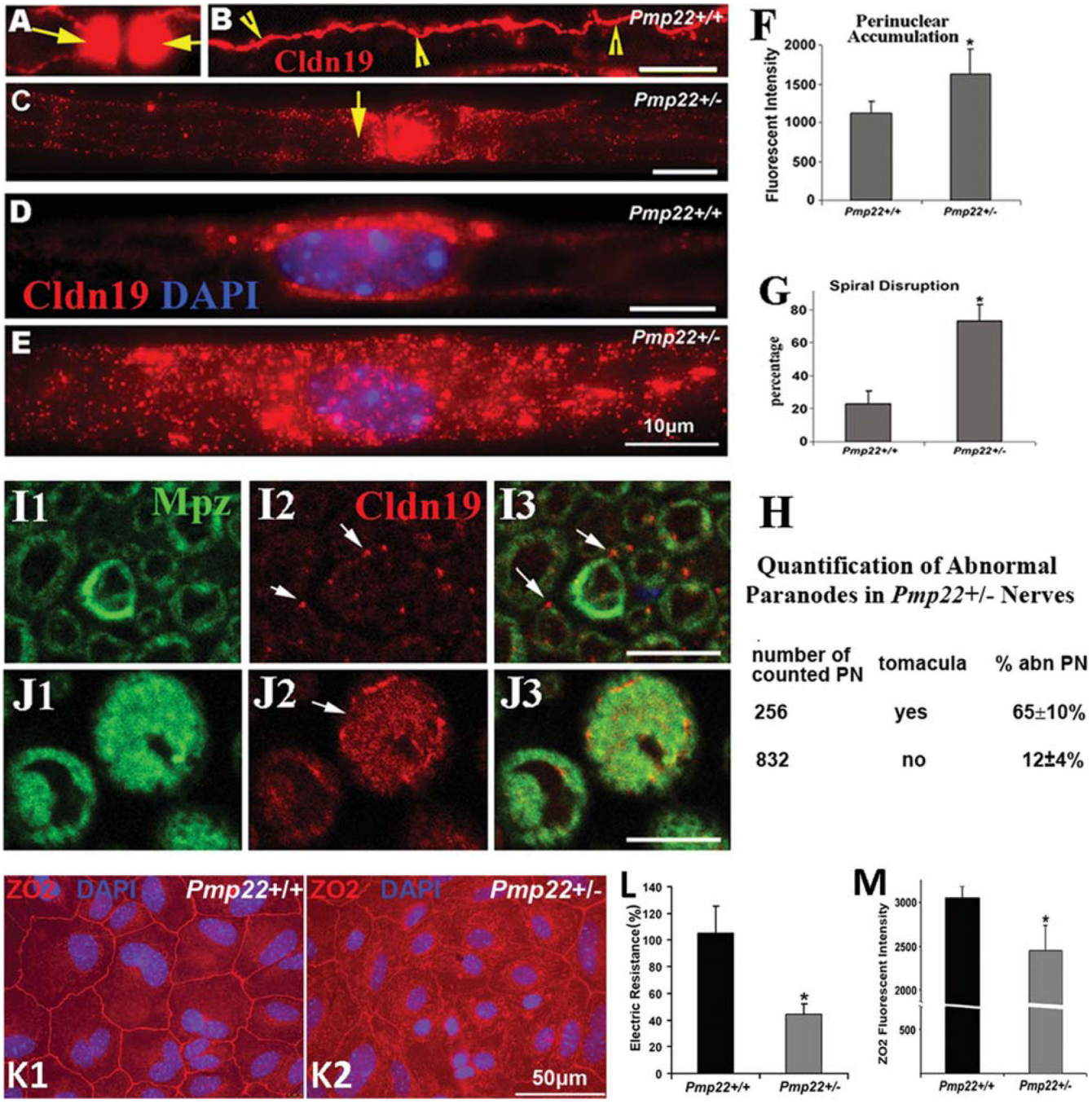

FIGURE 3.

Alterations of tight junction protein complex in *Pmp22*$^{+/-}$ myelinated nerve fibers. Sciatic nerves from 10-monthold mice (n = 5 *Pmp22*$^{+/+}$ and 5 *Pmp22*$^{+/-}$ mice) were teased into individual fibers and stained with antibodies against claudin-19. (A) Claudin-19 was strongly expressed in a pair of *Pmp22*$^{+/+}$ paranodes *(arrows)*. The paranodal signals had to be overexposed to visualize claudin-19 in other compartments. (B) Claudin-19 in the outer mesaxon tight junctions of a *Pmp22*$^{+/+}$ myelinated nerve fiber spirals along the internode *(arrowheads)*. (C) The mesaxon spirals and paranodal claudin-19 *(arrow)* were often reduced

or absent in the *Pmp22*$^{+/-}$ nerve fibers. (D) Mild accumulation of claudin-19 was occasionally visible in the *Pmp22*$^{+/+}$ Schwann cell perinuclear area. (E) This accumulation was severe in many *Pmp22*$^{+/-}$ perinuclear regions and extended into internodes in some fibers. (F) We measured the fluorescence intensity in the nuclear region, plus 2 areas flanking the nucleus, each with the length of one-half the nuclear diameters. There was a significant increase in *Pmp22*$^{+/-}$ mice (n = 5), compared with that in *Pmp22*$^{+/+}$ mice (n = 5; *t* test, $*p < 0.01$). (G) Internodes were analyzed quantitatively for disrupted spirals (discontinuous or absent). Their number was significantly increased in *Pmp22*$^{+/-}$ nerve fibers, compared to that in *Pmp22*$^{+/+}$ nerve fibers (n = 5 mice per group, *t* test, $*p < 0.01$). (H) Teased nerve fibers from 5 *Pmp22*$^{+/-}$ mice were counted to calculate percentages of paranodes with abnormal claudin-19 distribution, including absent or severely decreased paranodal claudin-19 bands and disrupted mesaxon spirals. Percentages of abnormal paranodes (abn PN) were compared between paranodes with tomacula and paranodes without tomacula. These abnormal paranodes were not found in *Pmp22*$^{+/+}$ nerve fibers. (I1–3) Transverse sections of paraffin-embedded sciatic nerves from *Pmp22*$^{+/+}$ mice were double-stained with antibodies against Mpz and claudin-19. As demonstrated previously (Fig 6 in Miyamoto et al[30]), a transected spiral of claudin-19 in the inner or outer mesaxon appeared as dots (*arrows* in I2, I3). Claudin-19 accumulated on *Pmp22*$^{+/-}$ myelin of some tomacula (*arrow* in J2) and lost its dotlike appearance. (K1) Primary epithelial cell culture from *Pmp22*$^{+/+}$ mouse renal medullar tubules was stained with antibodies against zonula occludens 2 (ZO2) to show intercellular tight junctions. (K2) In *Pmp22*$^{+/-}$ cells, there were many islands where tight junctions were disrupted. (L) The electrical resistance of tight junctions was measured. All raw values of the resistance were normalized to that from simultaneously cultured wild-type cells[32] and expressed as percentages on the y-axis. The mean electrical resistance was calculated from 19 *Pmp22*$^{+/+}$ cultures (12 mice) and 20 *Pmp22*$^{+/-}$ cultures (10 mice). There was a significant reduction of the resistance in *Pmp22*$^{+/-}$ epithelial cell tight junctions, compared with that in *Pmp22*$^{+/+}$ cells (*t* test, $*p < 0.01$). (M) The images described in K1–2 were divided by 3 vertical lines. Any junctions that ran across the vertical lines were quantified for their fluorescence intensity. Values of the intensity either from *Pmp22*$^{+/+}$ or *Pmp22*$^{+/-}$ cultures showed a significant decrease of ZO2 expression in the *Pmp22*$^{+/-}$ tight junctions (n = 10 cultures for each group; *t* test, $*p < 0.05$).

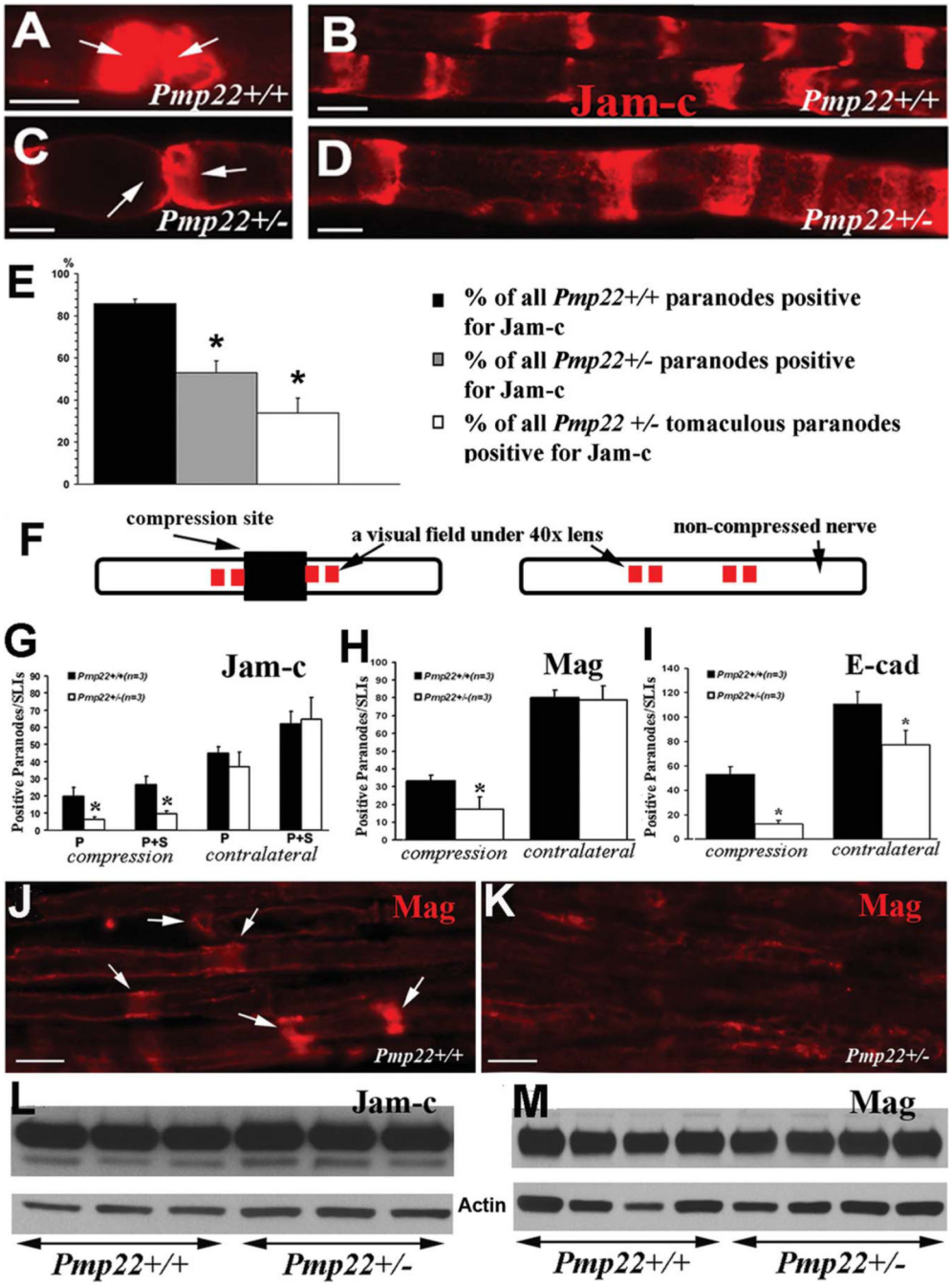

FIGURE 4.

Abnormal expression of transmembrane adhesion proteins. (A) Sciatic nerves from 5-month-old mice were teased into individual nerve fibers. A pair of *Pmp22*$^{+/+}$ paranodes *(arrows)* were strongly stained by antibodies against Jam-c. (B) The *Pmp22*$^{+/+}$ internodes contained Schmidt–Lanterman incisures (SLIs) that were stained by Jam-c. (C) Jam-c was decreased or missing in *Pmp22*$^{+/-}$ paranodes *(arrows)*. (D) Jam-c pattern in *Pmp22*$^{+/-}$ SLIs appeared to be unchanged. (E) Percentages of paranodes positive for Jam-c were manually counted in teased nerve fibers from 3 *Pmp22*$^{+/+}$ and 3 *Pmp22*$^{+/-}$ mice. The percentage was

decreased in *Pmp22*$^{+/-}$ paranodes either with or without tomacula (*$p < 0.05$). (F) This diagram shows the experimental approach for data in G–K. Sciatic nerves in 3-month-old mice were compressed for 30 minutes using a vessel clamp.[8] The nerves were dissected to be embedded in paraffin. The longitudinal paraffin sections were stained with antibodies against Jam-c or Mag. The compressed region is marked by a dark rectangular box. Red squares immediately adjacent to the compression site represent 4 fields imaged under a ×40 lens. All quantifications were reported in G–I. (G) Paranodes/SLIs positive for Jam-c were counted and showed no significant difference between 3-month-old *Pmp22*$^{+/+}$ and *Pmp22*$^{+/-}$ mice (n = 3 mice for each group). However, after compression, there were fewer Jam-c–positive paranodes/SLIs in *Pmp22*$^{+/-}$ nerves than in *Pmp22*$^{+/+}$ nerves. To avoid any false counting in paranodes/SLIs that were deformed by compression, any partially stained structures were not included in counts. P = paranodes; P1S = paranodes1SLIs (n = 3 mice for each group; analysis of variance, *$p < 0.05$). (H) A similar change was found for Mag (n = 3 mice for each group; *t* test, *$p < 0.05$). (I) For E-cadherin (n = 3 mice for each group; *t* test, *$p < 0.05$), the difference between *Pmp22*$^{+/-}$ and *Pmp22*$^{+/+}$ nerves was found in either noncompressed or compressed nerves. (J) A *Pmp22*$^{+/+}$ nerve section was stained by Mag antibodies after the nerve compression. A portion of Mag-positive SLIs were still visible. (K) In contrast, Mag-positive SLIs were hardly detectable in a *Pmp22*$^{+/-}$ nerve section after the compression. (L, M) Jam-c and Mag levels by Western blot analysis were not different between naive *Pmp22*$^{+/+}$ and *Pmp22*$^{+/-}$ nerves (densitometry measurements: Jam-c = 0.85±0.06 in *Pmp22*$^{+/+}$ vs 0.81±0.03 in *Pmp22*$^{+/-}$, n = 5 mice for each group, *t* test, $p = 0.27$; Mag = 0.75±0.06 vs 0.78±0.05, n = 9 mice for each group, *t* test, $p = 0.70$). Actin bands were the loading controls. All scale bars = 10lM.

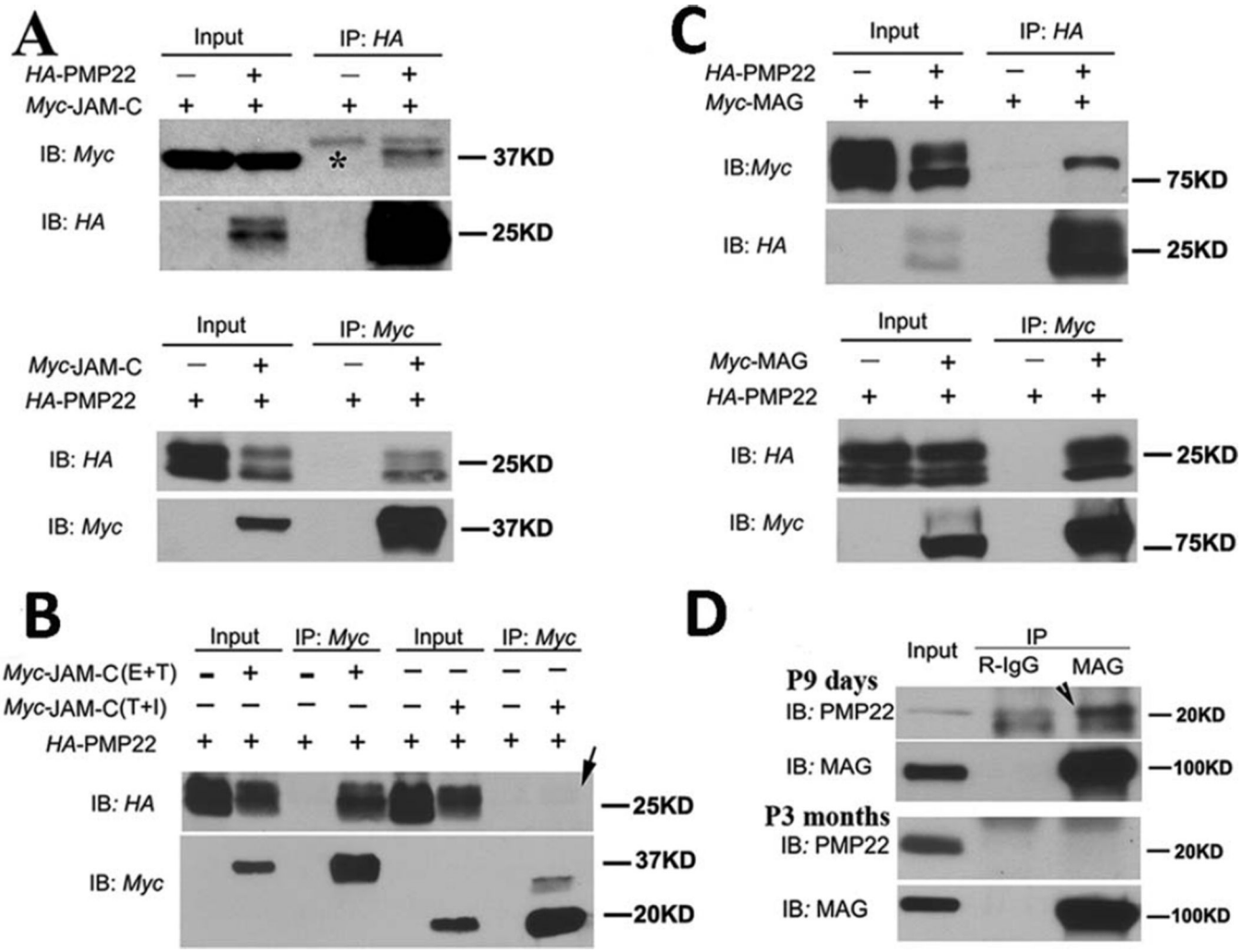

FIGURE 5.

Interactions between PMP22 and immunoglobulin (Ig) domain proteins. (A) Coexpression of human PMP22 and 1 of the Ig domain proteins (JAM-C) was done in HEK293a cells. Ten percent of cell lysates were loaded as inputs and blotted with the anti-Myc or anti-HA antibodies (Input lanes). The remaining lysates were subjected to immunoprecipitation with 1 of the 2 antibodies (Myc and HA). The precipitated proteins were detected by immunoblotting with antibodies (IP lanes). *Heavy chain of immunoglobulin in A. IB = immunoblotting; IP = immunoprecipitation. (B) Two JAM-C mutants were respectively coexpressed with PMP22. JAM-C with an intracellular domain deletion was still able to pull down PMP22. However, JAM-C with a deletion of extracellular Ig domain failed to pull down the PMP22 (*arrow* in lane *8*). E = extracellular domain; I = intracellular domain; T = transmembrane domain. (C) The same coimmunoprecipitation experiments were done to detect the interaction between PMP22 and MAG in HEK293a cells. (D) To examine interactions between endogenous PMP22 and MAG, lysates were extracted from mouse sciatic nerves at postnatal day 9. Mag antibodies were able to pull down endogenous Pmp22 *(arrowhead)*, but failed to do so in 3-month-old nerves.

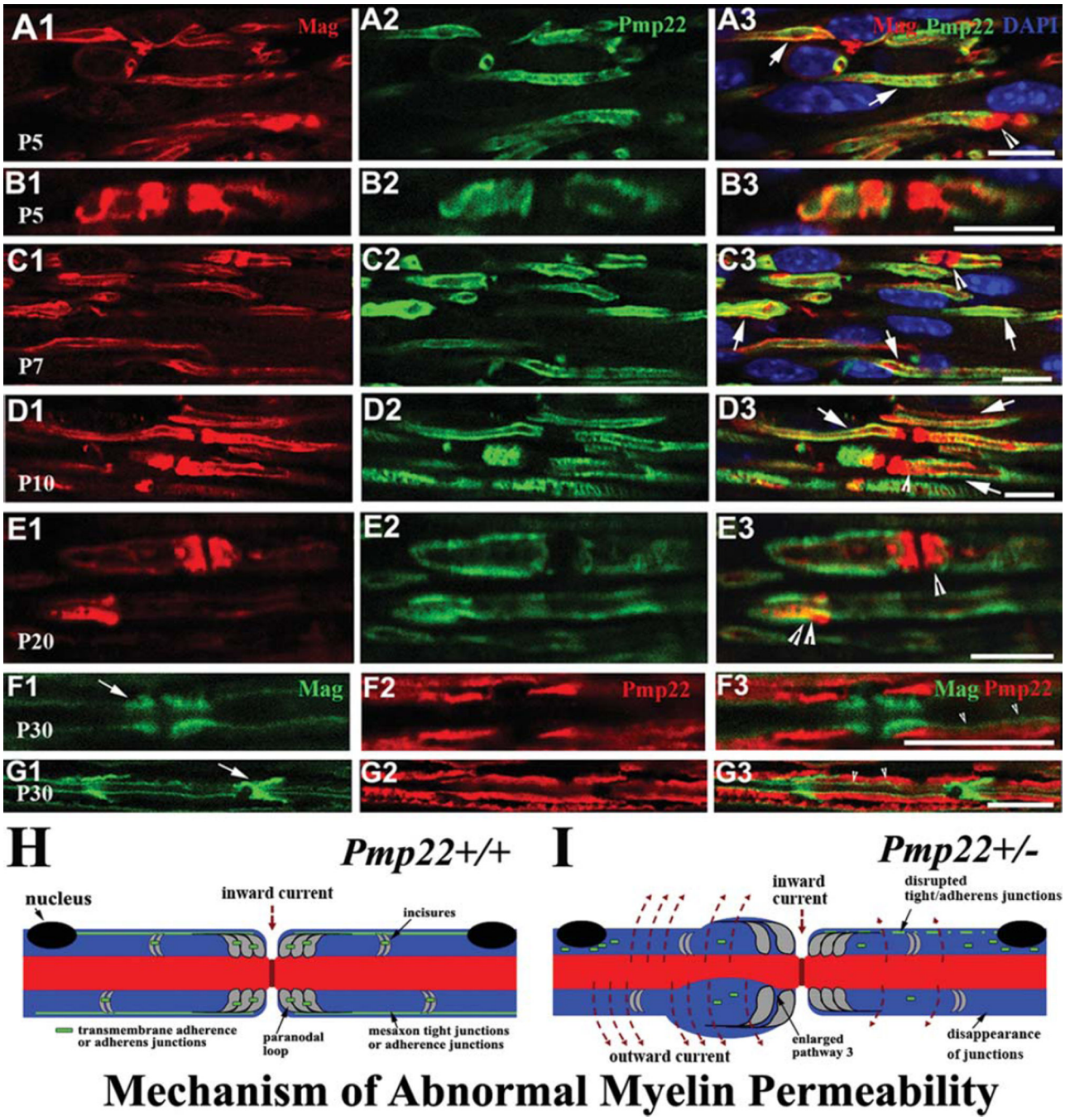

FIGURE 6.

Colocalization between Pmp22 and Mag during development. (A1–3) Wild-type sciatic nerves at postnatal day 5 (P5) were embedded in paraffin. Nerves were cut into longitudinal sections and stained with antibodies against Pmp22 and Mag. Both Pmp22 and Mag were distributed in the immature internodes and often overlapped (*arrows* in A3). Paranodes positive for Mag were detectable (*arrowhead* in A3). Pmp22 was seen in some premature paranodes and overlapped with Mag (*arrowhead* in A3). (B1–3) Another pair of P5 paranodes contained the colocalized Pmp22 and Mag. Notice that Pmp22 was overlapped

with Mag in nearly the entire paranode on the left, but only partially occupied the paranode on the right. (C1–D3) These colocalizations were also found in P7 and P10 mouse nerves (*arrows* or *arrowheads* in C3 or D3). (E1–3) By P20, Pmp22 and Mag were better confined into internodal compact myelin and noncompact regions. However, a partial overlapping of the 2 proteins was still detectible in a paranode (*single arrowhead* in E3) and Schmidt–Lanterman incisure (SLI; *double arrowheads* in E3). (F1–G3) By P30, Pmp22 and Mag were well separated. Pmp22 was in internodal compact myelin (F2 and G2). Mag was restricted into paranodes (*arrow* in F1), SLIs (*arrow* in G1), and inner mesaxons (*arrowheads* in F3 and G3). (H, I) Diagrams show our proposed mechanisms. (H) Myelin junctions in *Pmp22*$^{+/+}$ nerve are depicted in paranodes, SLIs, and mesaxons. These junctions prevent axonal current from leaking out. (I) Nerve fiber with Pmp22 deficiency develops a tomacula in the left paranode, but no demyelination. However, junction protein complexes are disrupted or disappeared in paranodes, SLIs, and/or mesaxons. These junction proteins may be found in aberrant locations, including perinuclear regions or tomaculous myelin. Abnormal assembly of these junctions in Pmp22 deficiency loosens adhesion between myelin lamellae and between other myelin junctions, thereby increasing myelin permeability without demyelination. Notice that pathway 3 is demarcated by 2 adjacent paranodal loop laminae and axolemma. Therefore, pathway 3 is subject to the regulation of transmembrane adhesion proteins, such as Jam-c.[17] Pathway 3 is likely enlarged to increase myelin permeability in *Pmp22*$^{+/-}$ nerve.